Arab J Geosci (2015) 8:2347–2357
DOI 10.1007/s12517-014-1380-4

ORIGINAL PAPER

Site response assessment of an urban extension site using microtremor measurements, Ahud Rufeidah, Abha District, Southwest Saudi Arabia

Sattam Almadani · Kamal Abdelrahman · Elkhedr Ibrahim · Abdulaziz Al-Bassam · Awad Al-Shmrani

Received: 18 November 2013 / Accepted: 17 March 2014 / Published online: 4 April 2014

Abstract Microtremor horizontal-to-vertical spectral ratio (HVSR) method has been conducted at 33 sites in Ahud Rufeidah urban expansion zone in order to assess the fundamental frequency and the corresponding amplitude of the sediments. Clear HVSR peaks have been identified in the majority of the surveyed area. The eastern and northern parts of the area are characterized by two well-separated peaks which indicate distinct shallow and deep impedance contrasts. The frequency map of sediments shows a distribution in the range of 0.86–3.13 Hz. The observed frequencies can be related to the total thickness of Quaternary alluvial sediments (sand, gravel, and shale) deposited over the gneiss bedrock. Lower resonance frequencies are attained at sites in the northern part, while the higher values are attained at sites in the southern part. The amplitudes of HVSR peaks are in the range 3–15. In general, the higher peak amplitudes are identified at lower frequencies. Since low fundamental frequencies are related to bedrock, this can be an indication of high-impedance contrast between alluvial sediments and gneiss bedrock. The results of this study represent one step for seismic hazard assessment and risk mitigation of this urban area where great damage can be attained in case of strong earthquakes. Hence, these results should be taken into consideration before establishing the new urban constructions in the area of study.

Keywords Site response · Urban zone · Fundamental frequency · Maximum amplitude

S. Almadani · K. Abdelrahman (✉) · E. Ibrahim · A. Al-Bassam · A. Al-Shmrani
Geology and Geophysics Department, College of Science, King Saud University, Riyadh, Kingdom of Saudi Arabia
e-mail: ka_rahmaneg@yahoo.com

A. Al-Bassam
Geology and Geophysics Department, College of Science, King Saud University, Riyadh, Kingdom of Saudi Arabia

E. Ibrahim
Geology Department, Faculty of Science, Mansoura University, Mansoura, Egypt

K. Abdelrahman
Seismology Department, National Research Institute of Astronomy and Geophysics, Helwan, Cairo, Egypt

Introduction

The local geology and topography can significantly control the scale and distribution of damages due to strong earthquakes. The maximum amplitude of earthquake ground motion by local site conditions has important implications in urban planning and development. In areas characterized by soft sediments, the maximum amplitude of ground motion is common that lead to enhanced seismic hazard and risk.

Local site response can be evaluated by empirical and theoretical methods. The theoretical method allows detailed analysis of the parameters used in the evaluation; however, it requires detailed geotechnical information about the materials through which the seismic waves propagate to the surface. Empirical methods are based on seismic records of the sites; thus, fundamental frequency and amplitude are determined directly. Empirical methods can be separated in two categories: one that uses two sites and another that uses only one site.

The approach of Borcherdt (1970), in which ambient seismic noise instead of earthquake is used, has been applied to several studies (Ohta et al. 1978). For frequencies smaller than 0.5 Hz, seismic noise is categorized as microseisms and, for higher frequencies, as microtremors. The main advantage given by this approach is that the spectral characteristics of microtremors have been recognized to be associated with the site conditions (Katz

1976; Katz and Bellon 1978; Kagami et al. 1986; Gutierrez and Singh 1992; Bard 2000). It has been shown that, with microtremors, it is possible to identify the fundamental resonance frequency of the near-surface soil deposits.

Nakamura (1989) proposed a method that requires only one recording station. Nakamura hypothesized that site response could be estimated from the horizontal-to-vertical ratio of microtremors. This technique was tested, experimentally and theoretically, at many sites all over the world, by different authors (Lermo and Chavez-Garcia 1993, 1994; Lachet and Bard 1994; Field and Jacob 1995; Malagnini et al. 1996; Seekins et al. 1996; Teves-Costa and Bard 1996; Theodulidis et al. 1996; Konno and Ohmachi 1998; Mucciarelli 1998; Mucciarelli et al. 1998). Results were obtained by implementing Nakamura's technique support of such use of microtremors measurements for estimating the site response of surface deposits. Lermo and Chavez-Garcia (1993) applied Nakamura's technique to seismic recordings of earthquakes and concluded that this approach is able to reliably estimate the frequency of the fundamental resonant mode and correctly predict the amplitude level. Other studies (Field and Jacob 1993; Wakamatsu and Yasui 1996; Lachet and Bard 1994) indicate that Nakamura method has already proved to be one of the cheapest and most convenient techniques to reliably estimate fundamental frequency, but it needs more work to understand the factors influencing the amplitude (Bard 2000).

Fnais et al. (2010) applied HVSR method for Yanbu City in Saudi Arabia along the Red Sea eastern coast. The estimated values of fundamental frequency range from 0.25–7.9 Hz, where these values increase with the decreasing depth to the bedrock.

Geological setting

The investigated site is called Wadi Al-Rubah to the southeast of Ahud Rufeidah at the southern border of the Abha District. The site is located between latitudes 18°11′00″ N and 18°11′41″ N and longitudes 42°51′49″ E and 42°52′28″ E, as shown in Fig. 1. Geologically, the study area lies on the southwestern edge of Asir Mountains, where surface dips gently due northeast away from the Red Sea escarpment. The basement rocks exposed in the study area represent the deepest erosional level

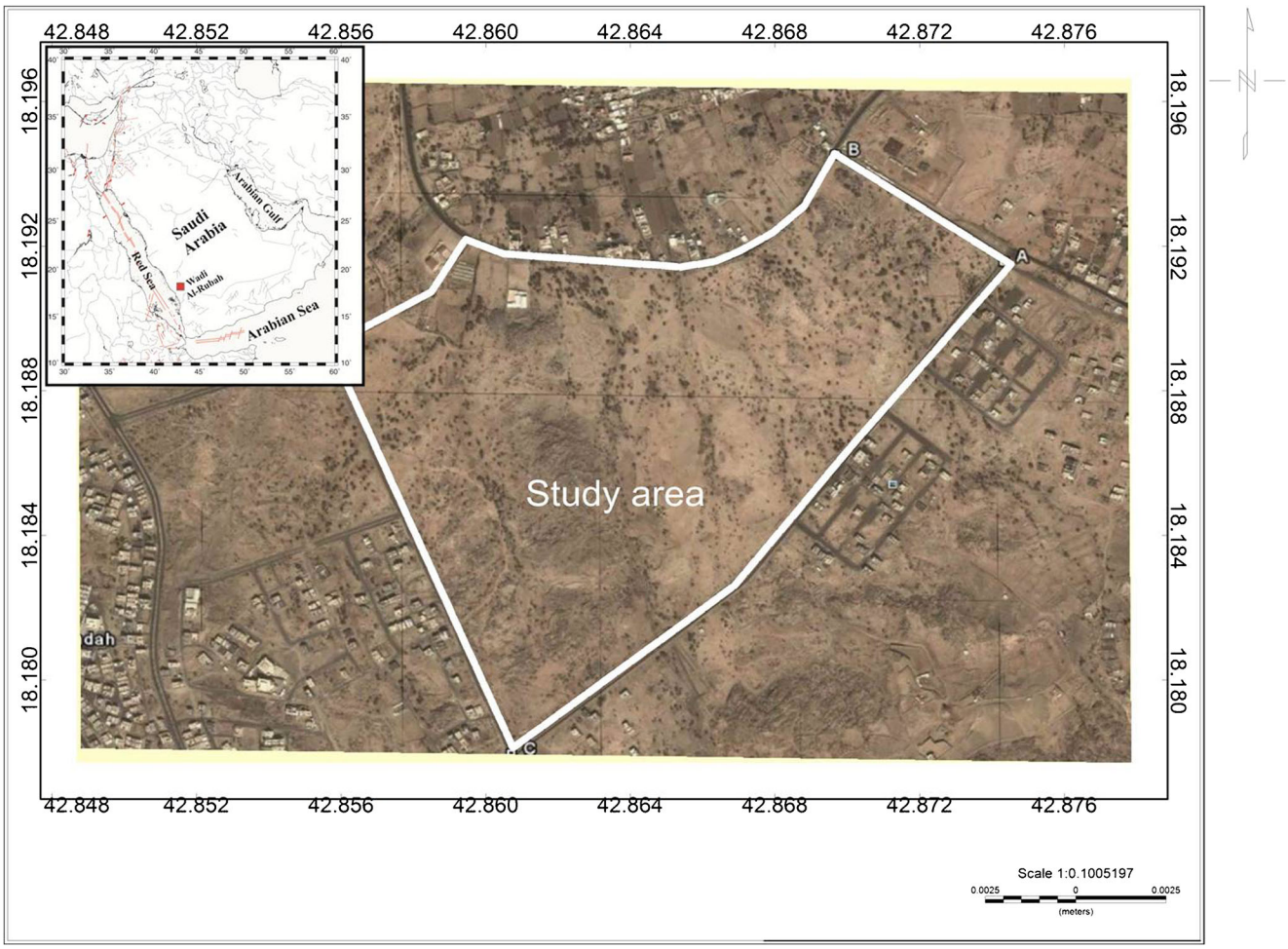

Fig. 1 Location map of the study area

of the Arabian Shield (Fig. 2). These basement rocks are divided into two distinct units:

1. Khamis Mushayt Gneiss: that composed of banded orthogneiss, migmatite with minor amphibolite, and paragniess.
2. Pegmatite: Numerous pegmatite and aplite dikes invaded the Khamis Mushayt Gniess, and their resistance to erosion has produced an erosional surface characteristic of the basement. It is composed of quartz, orthoclase, plagioclase and biotite.

These two basement units are covered in some localities with heterogeneous and spatially variable alluvial sediments. These sediments are composed of pebbles, gravels, sands, and clays that collected, transported, and deposited by running water into incised networks of narrow and active channels distributed across the floor of Ahud Rufaidah basin. The presence of such small and narrow channels could be referred to the underlying weathered easily eroded gneiss basement rocks and, consequently, increase in the channel depth and velocity. The basement gneiss and pegmatite rocks are covered with dry bed of slop-wash deposits with varying thicknesses that has been transported down a slope by mass wasting assisted by running water from the upstream and surrounding weathered gneiss and pegmatite hills. Structurally, left lateral strike–slip fault, right lateral strike–slip fault, joints, asymmetric anticline folds, similar folds, dikes, veins, and venlets structurally characterize the area. Tertiary normal faulting related to volcanism and development of the Red Sea depression is the latest structural events recorded (Coleman and Brown 1971).

Aim of study

The site response assessment usually gives detailed information about the nature and properties of the bedrock and overburden that can significantly control the scale and distribution of damages due to strong earthquakes. In the present study, the microtremor horizontal-to-vertical spectral ratio (HVSR)

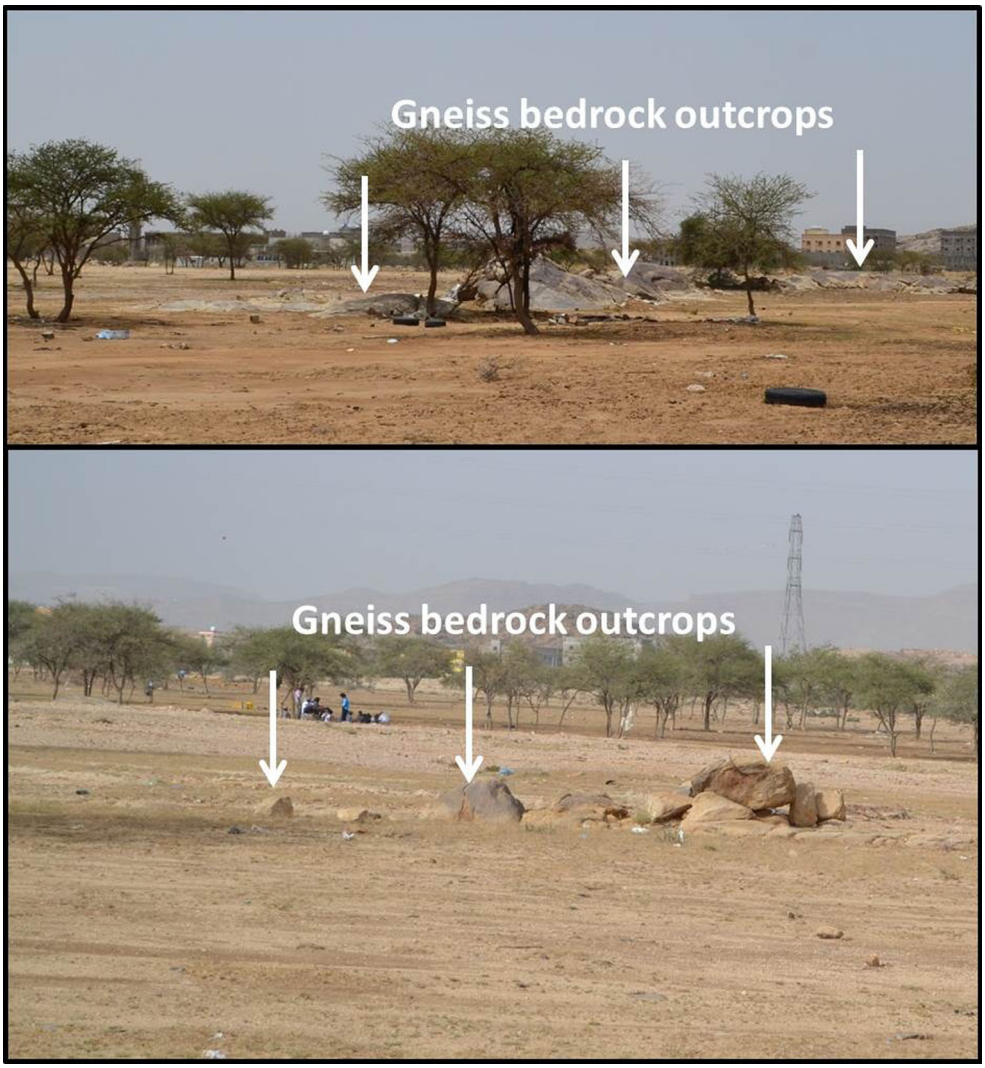

Fig. 2 Geologic setting of the study area

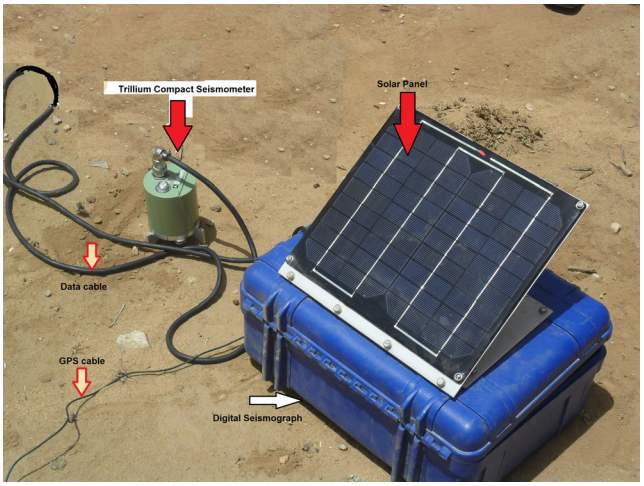

Fig. 3 Microtremor recording instruments

method has been applied on a site that represents an urban extension for the city of Ahud Rufeidah to the south of Abha District in order to assess the fundamental frequency (F_0) and the corresponding amplitude (A_0) of the sediments. This study has important application in urban planning and development as a tool of seismic hazard and risk mitigation.

Methodology

Instruments

Taurus data logger

The Taurus portable seismograph (Fig. 3) is a compact, self-contained digitizer and data logger that combines exceptional performance with versatility and low-power consumption. The Taurus can be used either as a stand-alone time series data logger or as a component in a data acquisition network. Taurus incorporates a three-channel 24-bit digitizer, GPS receiver and system clock, removable data storage, and remote communication options. Taurus is configurable locally using the color display screen and integrated browser or remotely using any web browser over a TCP/IP connection. Taurus is equipped with three 24-bit data channels. Time series data are stored in Steim (1) format and can be extracted to MiniSEED, Seisan, or ASCII format and streamed in Nanometrics NP format. Taurus supports 10/100Base-T Ethernet and serial interfaces.

As a portable unit, Taurus can be deployed to record continuous data for extended periods. For example, when recording three channels at 100sps, up to 600 days of data can be

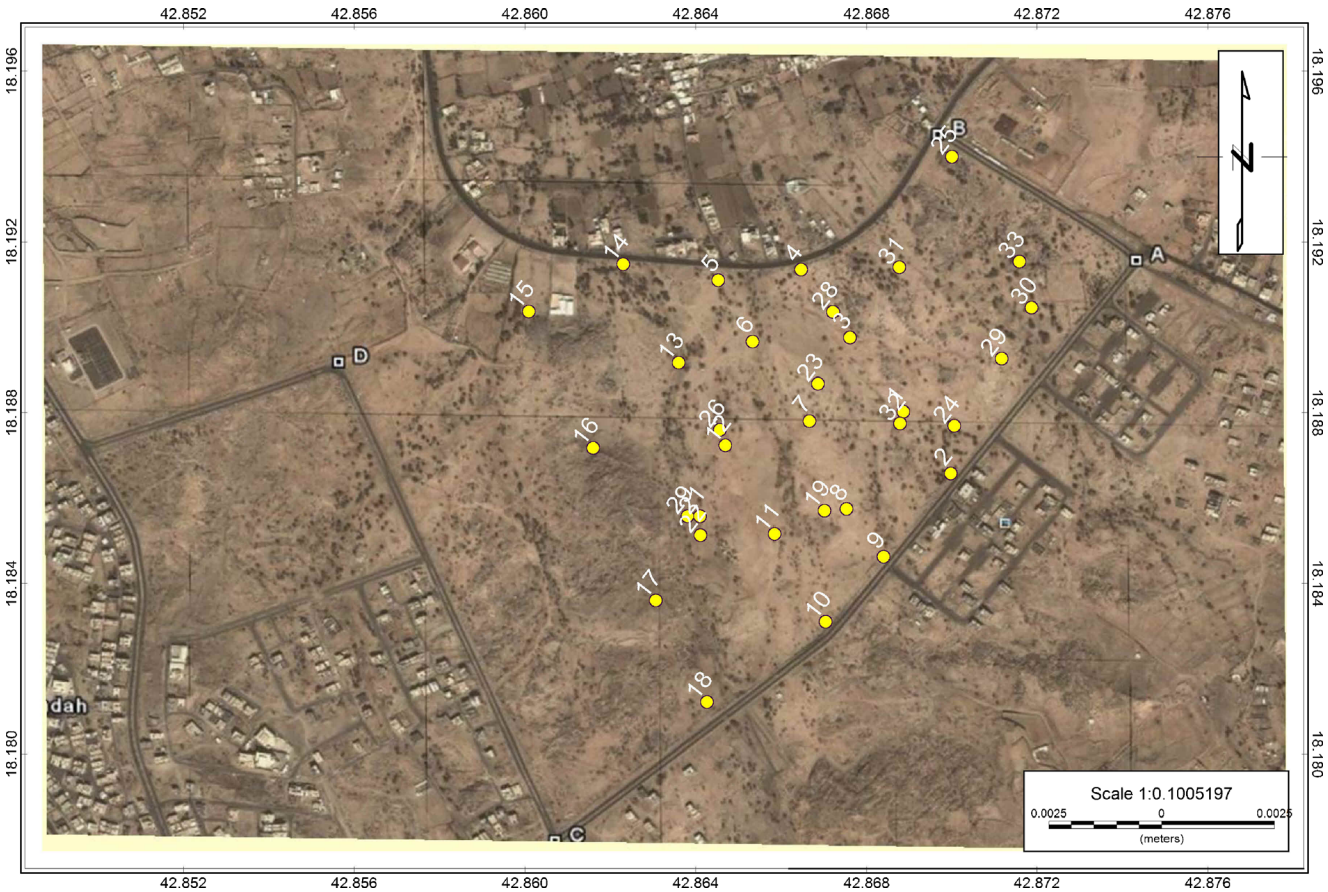

Fig. 4 Location map for measuring points

recorded using a 40 GB 1.8″ hard disk drive. A compact flash card may also be used as an alternative to a hard drive, for example, to use at more extreme temperatures or altitudes, or to realize optimal power consumption. Media are removable for easy data retrieval from the field. The extensive storage combined with low-power consumption make the Taurus ideal for long-term unattended data acquisition.

Trillium compact

Standing at just 128 mm (5.04″) tall with a diameter of only 90 mm (3.54″), trillium compact combines the superior performance of a broadband seismometer with the installation convenience of a rugged geophone. The instrument incorporates a symmetric triaxial force feedback sensor with a response flat to velocity from 120 s to 100 Hz. Scientists no longer need to compromise on performance in applications demanding small, highly portable seismometers.

Data acquisition and processing

Microtremor field measurements

Microtremor measurements were acquired for 33 observation sites (Fig. 4). At each site, the microtremors were recorded continuously for almost 1 h. The microtremors have been recorded with the following precautions according to Nakamura

Table 1 Acquisition parameters of microtremor measurements at study area

Site code	Latitude (N)	Longitude (E)	Date	Start time	End time	Duration (minutes)	Sensor type	Sampling frequency
1	42:52:7.90	18:11:16.90	22/6/2013	05:40	06:20	40	T.C.	100
2	42:52:11.90	18:11:11.70	22/6/2013	06:50	07:30	40	T.C.	100
3	42:52:3.39	18:11:23.15	22/6/2013	07:58	08:38	40	T.C.	100
4	42:51:59.30	18:11:28.90	22/6/2013	08:58	09:38	40	T.C.	100
5	42:51:52.30	18:11:28.00	22/6/2013	10:00	10:40	40	T.C.	100
6	42:51:55.20	18:11:22.80 b	23/6/2013	04:02	04:32	30	T.C.	100
7	42:52:0.00	18:11:16.10	23/6/2013	04:55	05:35	40	T.C.	100
8	42:52:3.10	18:11:8.70	23/6/2013	06:00	06:30	30	T.C.	100
9	42:52:6.23	18:11:4.68	23/6/2013	06:55	07:25	30	T.C.	100
10	42:52:1.37	18:10:59.18	23/6/2013	08:40	09:10	30	T.C.	100
11	42:51:57.06	18:11:6.61	23/6/2013	09:41	10:11	30	T.C.	100
12	42:51:52.90	18:11:14.05	24/6/2013	04:24	04:54	30	T.C.	100
13	42:51:48.96	18:11:21.02	24/6/2013	05:17	05:57	40	T.C.	100
14	42:51:44.28	18:11:29.36	24/6/2013	06:02	06:42	40	T.C.	100
15	42:51:36.31	18:11:25.35	24/6/2013	06:50	07:30	40	T.C.	100
16	42:51:41.74	18:11:13.83	24/6/2013	07:45	08:20	35	T.C.	100
17	42:51:47.03	18:11:0.98	24/6/2013	08:55	09:30	35	T.C.	100
18	42:51:51.35	18:10:52.41	24/6/2013	09:55	10:35	40	T.C.	100
19	42:52:1.27	18:11:8.55	29/6/2013	05:10	05:50	40	T.C.	100
20	42: 51:49.7	18: 11:8.08	29/6/2013	06:10	06:50	40	T.C.	100
21	42:51:50.76	18:11:8.08	29/6/2013	07:10	07:50	30	T.C.	100
22	42:51:50.8	18:11:6.50	29/6/2013	08:00	08:30	30	T.C.	100
23	42:52:0.72	18:11:19.26	12/6/2012	08:10	08:58	48	T.C.	100
24	42:52:12.2	18:11:15.7	21/6/2012	06:20	06:50	30	T.C.	100
25	42:52:2.46	18:11:39	21/6/2012	07:15	07:45	30	T.C.	100
26	42:51:52.44	18:11:15.36	21/6/2012	08:13	08:43	30	T.C.	100
27	42:52:53.16	18:11:21.9	21/6/2012	09:21	09:52	32	T.C.	100
28	42:52:1.98	18:11:25.32	22/6/2012	10:18	10:49	31	T.C.	100
29	42:52:16.2	18:11:21.36	22/6/2012	04:17	04:47	30	T.C.	100
30	42:52:18.72	18:11:25.68	22/6/2012	05:08	05:42	34	T.C.	100
31	42:52:7.56	18:11:29.1	22/6/2012	06:00	06:30	30	T.C.	100
32	42:52:7.62	18:11:15.9	22/6/2012	07:05	07:35	30	T.C.	100
33	42:52:17.7	18:11:29.58	24/6/2012	05:40	06:40	60	T.C.	100

(1996), Mucciarelli et al. (1998), Mucciarelli (1998), and SESAME (2004): (i) Measurements were carried out using 1-s (or higher) triaxial velocimeter, for the analysis at periods longer than 1-s carried out measurements; (ii) Avoid long external wiring, for reducing any mechanical and electronic interference; (iii) Avoid measurements in windy or rainy days, which can cause large and unstable distortions at low frequencies; and (iv) Avoid recordings close to roads with heavy vehicles, which cause strong and rather long transients. All the abovementioned precautions in addition to the following guidelines should be read carefully before and during the field measurements.

Digital records were recorded with a sampling rate of 100 samples per second. Table 1 presents the time of measurements at various sites. The length of recording for each measurement is an important parameter where too short a period will result in unreliable average spectral ratios. The sensors used were calibrated before recording and installed in good coupling with soil. Furthermore, it was isolated thermally against temperature changes using thick foam box and covered to reduce the interference of wind. Then these sensors were oriented horizontally (northsouth and eastwest) and vertically leveled.

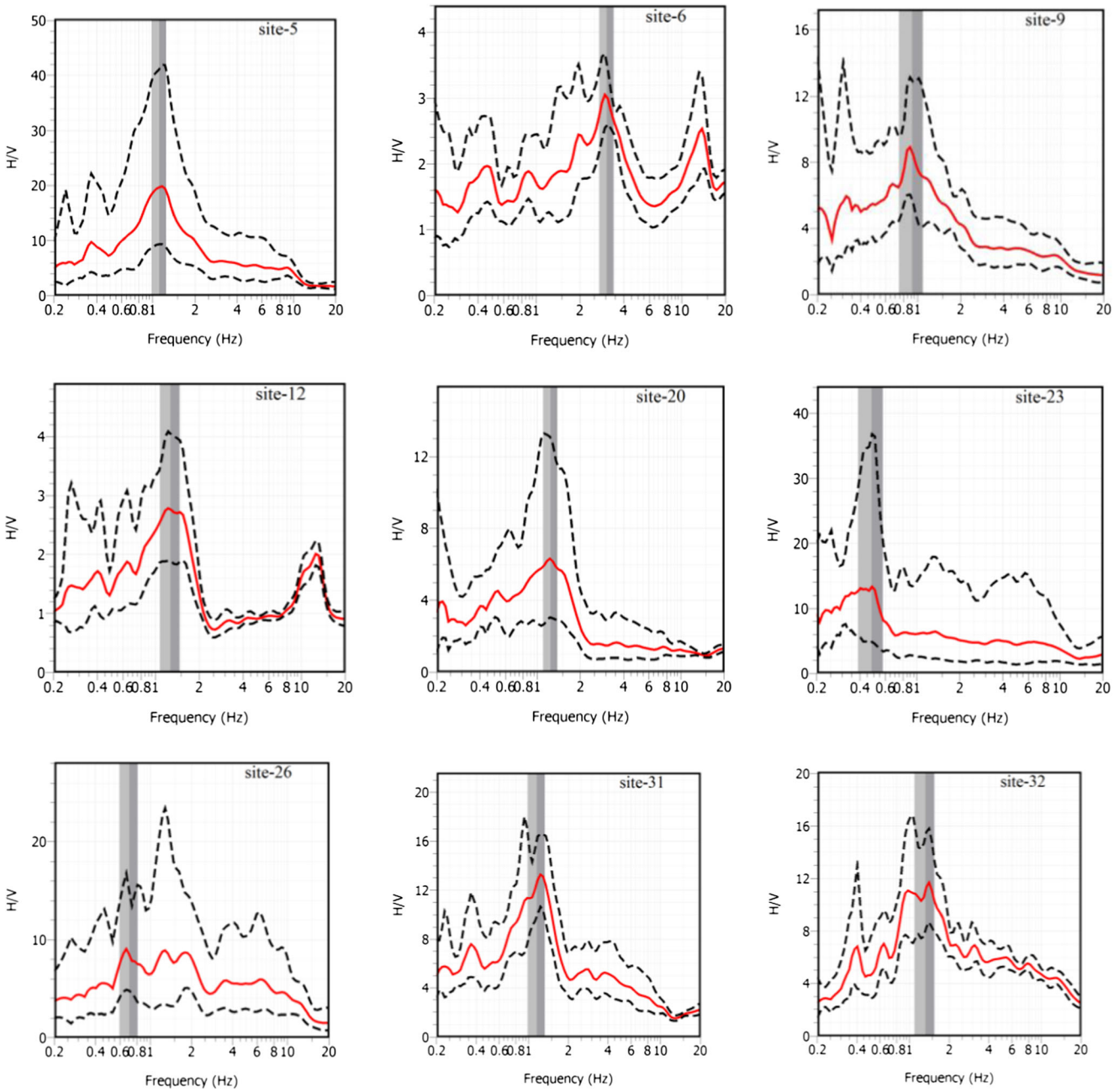

Fig. 5 Examples of microtremor results at the study area

Data processing

The collected data have been processed through Geopsy_software developed within the framework of the European project SESAME. At each site, the field measurements sheet proposed by SESAME project (SESAME 2004) was filled in terms of time, date, operator name, coordinates, etc. All the necessary and recommended information about the recorded signals were applied according to these guidelines.

At each site, the microtremors data file was divided into several time windows of 15–50 s for spectral calculations. This time window is proven sufficiently long to provide stable results. The selected time windows were Fourier-transformed using cosine tapering before transformation. The spectra were then smoothed with a Konno and Ohmachi algorithm (Konno and Ohmachi 1998). After data smoothing, the spectra of EW and NS channels at a site were divided by the spectra of the vertical channel (Nakamura estimate) in order to obtain spectral ratios. The geometrical average of the two component ratios is the site amplitude function. However, in most cases, due to the influence of sources like dense population, high traffic, and industry activities, the resonance frequency cannot be directly identified from microtremors spectra (Duval et al. 2004). Examples of the HVSR results are presented in Fig. 5. Fundamental frequencies and the corresponding amplitude from all measurement sites in the study area are summarized in Table 2. The origin of selected peaks is natural.

Table 2 Results of microtremor measurements

Site code	No. of samples	No. of windows (n_w)	Window length (l_w)	No. of cycles (n_c)	A_0	σ$A(f)$	F_0	σf
1	240,000	13	20	234	2.34	1.79	0.9	±0.11
2	240,000	10	25	275	6.0	1.35	1.1	±0.23
3	240,000	10	28	308	4.05	1.83	1.37	±0.06
4	238,604	10	18	228.6	8.63	1.69	1.27	±0.22
5	240,000	14	25	420	15.67	1.35	1.2	±0.13
6	180,000	18	30	1706	3.01	1.17	3.13	±0.35
7	175,000	10	27	297	2.63	1.79	1.1	±0.2
8	180,000	10	16	283.2	10.47	1.26	1.77	±0.22
9	168,500	14	25	301	8.57	1.5	0.86	±0.17
10	180,000	10	14	203	6.5	1.79	1.45	±0.34
11	180,000	11	22	300.1	6.13	1.67	1.24	±0.25
12	120,000	10	35	444.5	2.76	1.46	1.27	±0.19
13	120,000	12	50	699	6.0	1.57	1.16	±0.21
14	147,400	10	25	315	7.72	1.5	1.26	±0.19
15	150,000	10	25	307.5	10.04	1.51	1.23	±0.27
16	156,000	10	50	575	1.15	1.13	4.15	±0.18
17	150,000	15	25	570	4.97	1.56	1.52	±0.29
18	86,000	10	25	382.5	7.66	1.62	1.53	±0.31
19	240,000	11	35	450.5	4.18	1.41	1.17	±0.17
20	240,000	10	25	310	6.28	1.27	1.24	±0.14
21	240,000	11	25	228.25	13.64	1.47	0.83	±0.11
22	180,000	10	25	282.5	6.97	1.65	1.13	±0.22
23	298,600	10	50	240	13.3	1.71	0.48	±0.09
24	180,000	12	24	342.72	4.04	1.16	1.19	±0.2
25	162,000	10	25	245	10.89	1.36	0.98	±0.22
26	180,000	20	35	490	8.42	1.53	0.7	±0.11
27	186,000	10	15	283.5	1.05	1.33	1.89	±0.12
28	186,000	20	35	371	14.8	1.41	0.53	±0.1
29	180,000	22	15	297	1.33	1.78	0.9	±0.06
30	204,000	10	30	330	1.77	1.39	1.1	±0.28
31	180,000	11	30	376.2	12.59	1.28	1.14	±0.16
32	176,800	10	20	264	11.05	1.37	1.32	±0.23
33	355,000	10	25	310	15.53	1.15	1.24	±0.26

The SESAME project recommended several criteria for reliability of results as follows:

$$F_0 > 10/l_w$$

According to this condition, at the frequency of interest, there is at least ten significant cycles in each window. Although not mandatory, but if the data allows, it is always fruitful to check whether a more stringent condition (f_0>20 / l_w) can be fulfilled, which allows at least ten significant cycles for frequencies half the peak frequency and thus enhances reliability of the whole peak:

$$n_c(f_0) > 200$$

According to this condition, a large number of windows are needed. The total number of significant cycles: $n_c=l_w f_0$ is larger than 200 (which means, for instance, for a peak of 1 Hz, there are at least 20 windows of 10 s each, or, for a peak of 0.5 Hz, 10 windows of 40 s each). In case no window selection is considered, all transients are taken into account:

$$\begin{array}{lll} \sigma A(f) < 2 \text{ for } 0.5f_0 < f < 2f_0 & \text{if} & f_0 > 0.5 \text{ Hz, or} \\ \sigma A(f) < 3 \text{ for } 0.5f_0 < f < 2f_0 & \text{if} & f_0 < 0.5 \text{ Hz} \end{array}$$

This condition takes into account an acceptably low level of scattering between all windows.

Results and discussion

The microtremors measurements yield maps of the fundamental frequency (F_0) and the corresponding amplitude (A_0) of

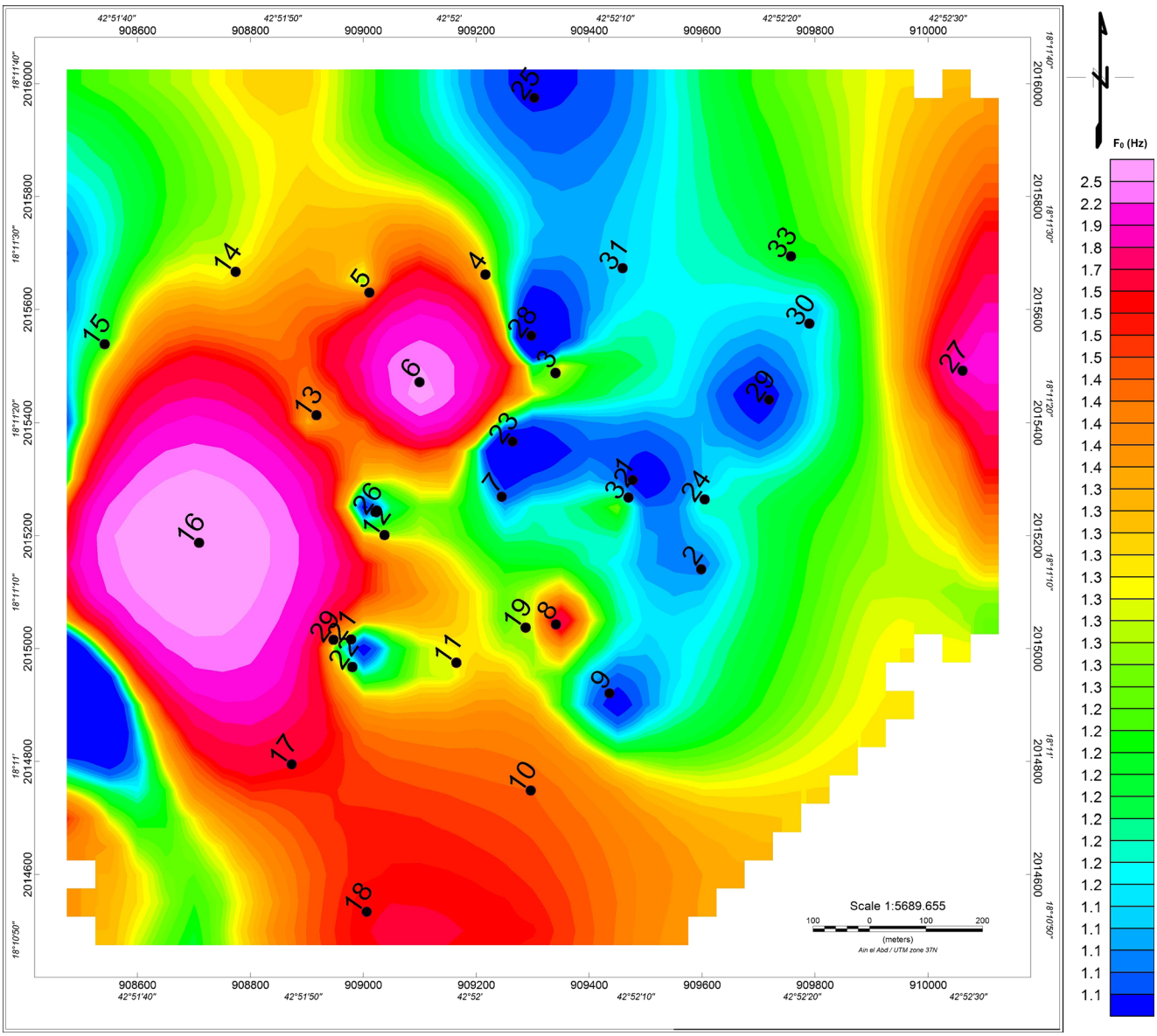

Fig. 6 The distribution of fundamental frequencies across the study area

ground motion (Figs. 6 and 7). The Fig. 6 created based on measured data shows a distribution of the fundamental frequency across the study area. The site response functions of the soil sites exhibit peaks at fundamental frequencies between 0.36 and 3.31 Hz. It is cleared from the map that the observed frequencies can be related to the total thickness of alluvial wadi-fill sediments. The lower resonance frequencies are attained at sites in the middle part of the investigated site, while the higher values are attained at the southwestern and eastern sides of the site with maximum value of about 3.31 Hz. These results indicate a shallow basement rock and, consequently, thinner sedimentary overburden in the southwestern and eastern sides; whereas there is thick, alluvial sediments overlie the basement gneiss rocks.

However, it is known that the amplitude of HVSR peak is a less reliable parameter of microtremor measurements (SESAME 2004). It can be therefore used only as a very rough indicator of impedance contrast between sediments and underlying bedrock. The map of maximum amplitude (Fig. 7) reflects a variation in the impedance values between the gneiss basement rock and the overlying alluvial sediments, where it ranges from 3 to 15. The highest amplifications are attained at the northern and eastern parts with relatively thick sediments, while the lower amplitude values are prevailed in the central part of the site with expected shallow basement rock. The intermediate values (around 7.3) of amplitude are encountered through the central part of the area.

In most cases, sharp peaks in HVSR, which are rather symmetrical (site 5, site 9, site 12, and site 31), have been identified. An asymmetrical shape with additional side peaks at frequencies lower than the frequency of the main peak is also clarified (site 6 and site 31). Some peaks are less sharp

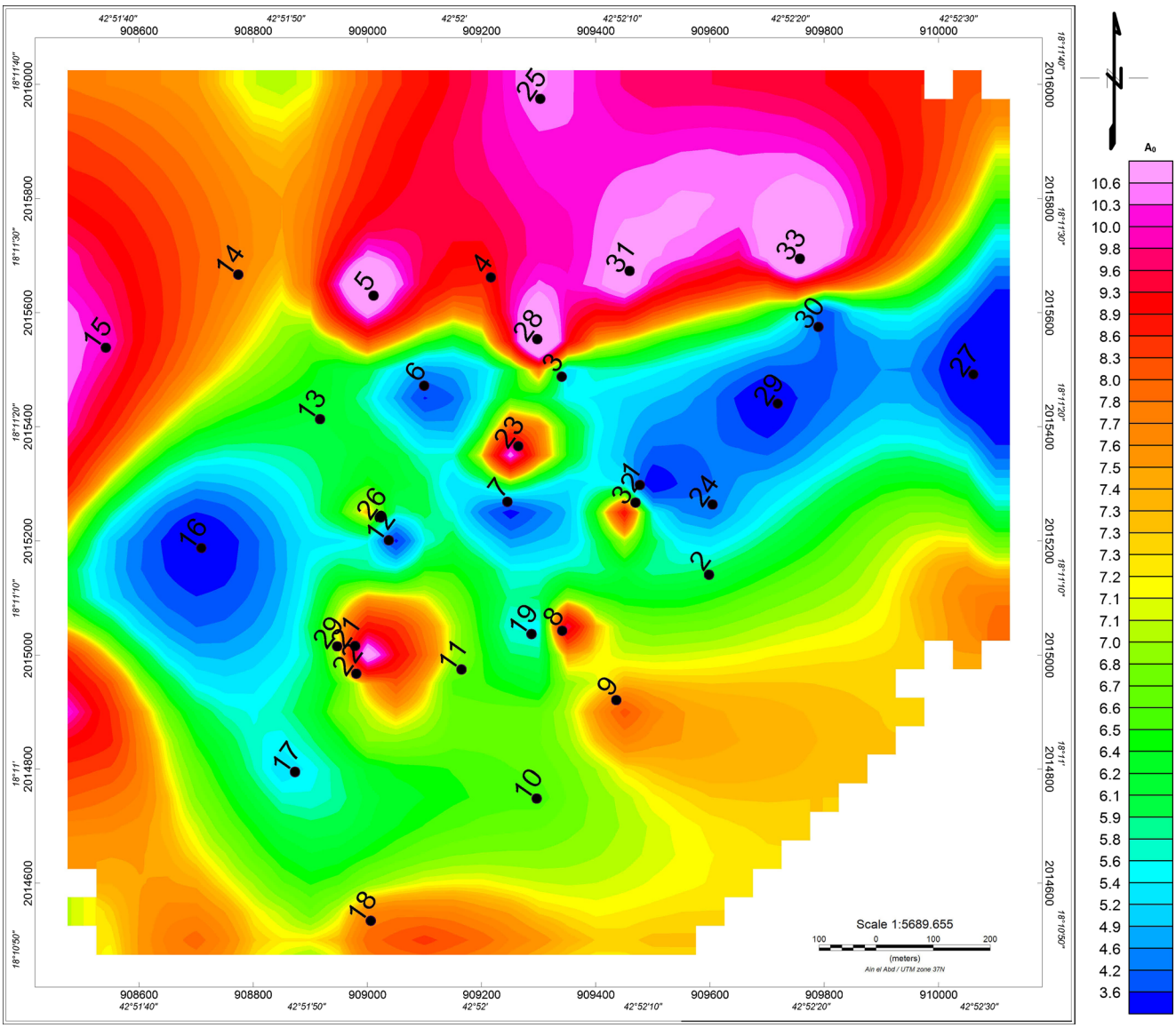

Fig. 7 The map of maximum amplitude across the study area

(site 26 and site 32) with some features, which can be an indication of two closely spaced peaks. Among shapes that are more complex, two peaks well separated in frequency (site 31) are defined. They indicate two impedance contrasts in the subsurface: first, shallow is most probably related to the sand and gravel layer, while the second, deep to the bedrock. Some measurements show several peaks (site 6 and site 26), indicating complex setting or broad peak. The lowest values of F_0 are indications for the thick sediments, while the higher values reveal thin section of sediments. This behavior indicates that there is heterogeneity or spatial variability in the thickness and properties of the sedimentary cover in the investigated site due to the presence of a thin layer of weathered loose gneiss beneath the alluvial sediments. Jamshidi et al. (2012) mentioned that the heterogeneity has significant effects in dynamic properties of natural alluvial deposits, and its negligence would result in an overestimation of the fundamental frequency of spatially variable alluvial deposits.

The amplitudes of HVSR peaks are in the range 3–15. In general, there are higher peak amplitudes at lower frequencies dominating the northern zone of the site, indicating the presence of thick alluvial deposits and deeper gneiss bedrock. Moving toward the south, the HVSR peaks indicate that the sedimentary cover gets thinner.

On the other hand, high fundamental frequencies are presumably related to parts where microtremor HVSR method detected shallower stiffer rocks within sediments. It is likely that the impedance contrast is, in this case, lower; nevertheless, more than one distinct impedance contrasts (as observed in site 6, site 31, and site 32). For measurements, which show two or more clear HVSR peaks, we used the value of the peak with higher amplitude.

Al-Haddad et al. (2001) indicated that site response frequencies less than 10 Hz are of engineering interest for 1-store reinforced concrete structures. Ahud Rufeidah urban expansion zone illustrates that the fundamental resonance frequencies in the range from 0.86 to 3.13 Hz, considering the relationship between the height of a building and its natural period of vibration, can be expressed as T=(number of stores) / 10. According to Parolai et al. (2006), it can be expected that in this urban area, the natural frequency of the soil matches the frequency of buildings with ≥one storey (Fig. 8). This means that, in Ahud Rufeidah urban zone, the natural frequency of the soil matches the frequency of buildings with ≥three stories. Most of the urban area characterized by low-rise buildings and the frequency of the soil cover can be close to their fundamental frequency of vibration.

This study represents a trial for seismic hazard assessment and risk mitigation where results will be of damaging effect in case of strong earthquakes, so it should be taken into consideration before construction of new urban settlements in the area of study.

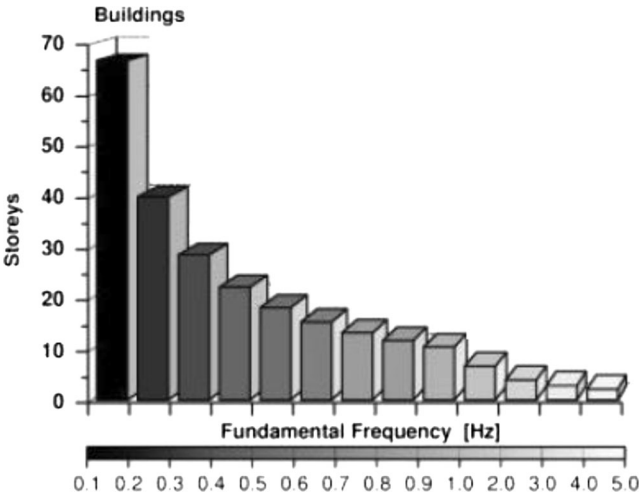

Fig. 8 Fundamental frequency of vibration of the buildings versus number of storeys in Cologne area, Germany (From Parolai et al. 2006)

Conclusions

Microtremor resonance frequency and spectral amplitude ratios have been calculated for urban extension area of Ahud Rufeidah city to the southwest of Saudi Arabia. Geologically the site consists of alluvial sediments (clays, sands, and gravel) of variable thicknesses overlie basement gneiss and pegmatite rocks.

A number of 33 microtremor measurements have been recorded to illustrate the variation of the fundamental frequencies and the corresponding amplitude in the area. The points of measurements were distributed in a pattern, which was designed to achieve good quality of the contour maps to show the distribution of the fundamental site frequency and amplitude.

The dataset, which has been processed using the horizontal-to-vertical spectral ratios (HVSR) that indicate thick alluvial cover, dominates the northern and eastern sides of the site with thinner thickness toward the center. The small circular and isolated high-amplitude anomalies could be related to bedrock, which is exposed at these localities in the center of the study area. The abrupt change in the thickness of the alluvial sediments to the northern side indicates the presence of a buried ENE-extended fault that controlled the abrupt change in the bedrock depth and, consequently, the thickness of the alluvial sediments. Another buried fault crosses the central part of the site and extends in the NNW direction (Figs. 5 and 6). These results indicate that present data can be correlated with the geological structures underlying the investigated site.

Finally, the obtained results of the present work will help in determining the amplitude characteristics of the investigated site. Such results when combined with the estimates of probable future earthquakes will help to approach the realistic hazard picture of the area.

Acknowledgments The authors extend their appreciation to the Deanship of Scientific Research at King Saud University for funding this work through research project no. NFG-14-03-25.

References

Al-Haddad M, Al-Rrefeai T, Al-Amri A (2001) Geotechnical investigation for earthquake resistance design in the Kingdom (phase 1) western coast. Research project no. AR-14-77 (part 1), funded by King Abdulaziz City for Science and Technology (KACST)

Bard PY (2000) International training course on: seismology, seismic data analysis, hazard assessment and risk mitigation, Potsdam, Germany, 01 October to 05 November 2000

Borcherdt RD (1970) Effects of local geology on ground motion near San Francisco Bay. Bull Seismol Soc Am 60:29–61

Coleman RG, Brown GF (1971) Volcanism in southwest Saudi Arabia. Geol Soc Am Abstr Programs 3:529

Duval A-M, Chatelain J-L, Guillier B, SESAME Team (Ricardo Azzara, Kuvvet Atakan, Pierre-Yves Bard, Sylvette Bonnefoy-Claudet, Fabrizio Cara, Cécile Cornou, Giovanna Cultrera, Donat Faeh, François Dunand, Philippe Guéguen, Mathilde Bøttger Sorens en, Johannes Ripperger, Paula Teves-Costa) (2004) Influence of experimental conditions on the H/V determinations using ambient vibrations (noise). Proceedings of the 13th World Conference on Earthquake Engineering. Paper No. 306, 1–6 August 2004, Vancouver, Canada

Field EH, Jacob KH (1993) The theoretical response of sedimentary layers to ambient seismic noise. Geophys Res Lett 20(24):2925–2928

Field EH, Jacob KH (1995) A comparison and test of various site-response estimation techniques, including three that are not reference-site dependent. Bull Seismol Soc Am 85:1127–1143

Fnais MS, Abdel-Rahman K, Al-Amri A (2010) Microtremor measurements in Yanbu City of western Saudi Arabia: a tool of seismic microzonation. J King Saud Univ Sci. doi:10.1016/j.jksus.2010.02.006

Gutierrez C, Singh SK (1992) A site effect study in Acapulco, Guerrero, Mexico: comparison of results from strong-motion and microtremor data. Bull Seismol Soc Am 82:642–659

Jamshidi R, Alinejad A, Davoodi M (2012) Uncertainty in fundamental natural frequency estimation for alluvial deposits. Comp Meth Civ Eng 3(1):77–94

Kagami H, Duke CM, Liang GC, Ohta Y (1986) Observation of 1- to 5-second microtremors and their application to earthquake engineering: Part II. Evaluation of site effect upon seismic wave amplification of deep soil deposits. Bull Seismol Soc Am 72:987–998

Katz LJ (1976) Microtremor analysis of local geological conditions. Bull Seismol Soc Am 66:45–60

Katz LJ, Bellon RS (1978) Microtremor site analysis study at Beatty, Nevada. Bull Seismol Soc Am 68:757–765

Konno K, Ohmachi T (1998) Ground-motion characteristics estimated from spectral ratio between horizontal and vertical components of microtremors. Bull Seismol Soc Am 88:228–241

Lachet C, Bard PY (1994) Numerical and theoretical investigations on the possibilities and limitations of the Nakamura's technique. J Phys Earth 42:377–397

Lermo J, Chavez-Garcia FJ (1993) Site effect evaluation using spectral ratios with only one station. Bull Seismol Soc Am 83:1574–1594

Lermo J, Chavez-Garcia FJ (1994) Are microtremors useful in site response evaluation? Bull Seismol Soc Am 84:1350–1364

Malagnini L, Tricarico P, Rovelli A, Herrmann RB, Opice S, Biella G, de Franco R (1996) Explosion, earthquake, and ambient noise recording in a Pliocene sediment-filled valley: inferences on seismic response properties by reference- and non-reference-site techniques. Bull Seismol Soc Am 86:670–682

Mucciarelli M (1998) Reliability and applicability of Nakamura's technique using microtremors: an experimental approach. J Earthq Eng 4:625–638

Mucciarelli M, Contri P, Monachesi G, Calvano G (1998) Towards an empirical method to instrumentally assess the seismic vulnerability of existing buildings. Proceedings of Conference on Disaster Mitigation and Information Technology, London

Nakamura Y (1989) A method for dynamic characteristics estimation of subsurface using microtremor on the ground surface. QR of RTRI 30(1):25–33

Nakamura Y (1996) Real-time information systems for seismic hazard mitigation UrEDAS, HERAS and PIC. QR of RTRI 37(3):112–127

Ohta Y, Kagami H, Goto N, Kudo K (1978) Observation of 1- to 5-second microtremors and their application to earthquake engineering: Part I. Comparison with long period accelerations at the Tokachi-Oki earthquake of 1968. Bull Seismol Soc Am 68:767–779

Parolai S, Richwalski SM, Milkereit C, Fah D (2006) S-wave velocity profiles for earthquake engineering purposes for the Cologne area (Germany). Bull Earthq Eng 4:65–94

Seekins LC, Wennerberg L, Margheriti L, Liu H-P (1996) Site amplification at five locations in San Francisco, California: a comparison of S waves, codas and microtremors. Bull Seismol Soc Am 86:627–635

SESAME (2004) Guidelines for the implementation of the H/V spectral ratio technique on ambient vibrations — measurements, processing and interpretations. SESAME European research project EVG1-CT-2000-00026 D23.12. http://sesame-fp5.obs.ujf-grenoble.fr

Teves-Costa MPL, Bard P-Y (1996) Seismic behavior estimation of thin alluvium layers using microtremor recordings. Soil Dyn Earthq Eng 15:201–209

Theodulidis N, Bard PY, Archuleta R, Bouchon M (1996) Horizontal-to-vertical spectral ratio and geological conditions: the case of Garner valley downhole in Southern California. Bull Seismol Soc Am 68:767–779

Wakamatsu K, Yasui Y (1996) Possibility of estimation for amplification characteristics of soil deposits based on ratio of horizontal to vertical spectra of microtremors. Proceedings of the 11th World Conference on Earthquake Engineering Acapulco. Mexico. Geophys Prospect 30:55–70